A DYNAMIC MODEL FOR SPACERS ON TRIPLE AND QUAD BUNDLES OF CONDUCTORS

László E. KOLLÁR, Masoud FARZANEH
NSERC/Hydro-Québec/UQAC Industrial Chair on Atmospheric Icing of Power Network Equipment (CIGELE) and Canada Research Chair on Atmospheric Icing Engineering of Power Networks (INGIVRE) at the University of Québec at Chicoutimi, Chicoutimi, Québec, Canada (www.cigele.ca)
laszlo_kollar@uqac.ca, farzaneh@uqac.ca

Abstract

A model is proposed to simulate the effects of high-amplitude vibrations on the spacer applied in triple and quad bundles of conductors. In particular, the model predicts the amplitude of vertical and transverse vibration at the attachment point of the spacer, the angle of spacer rotation, and thereby, the torsion of the bundle, and the magnitude of the force acting on the spacer during the vibration following ice shedding. The results are compared to those obtained for twin bundles in a recent research work; thus, this study predicts how the number of subconductors in a bundle affects the severity of vibration in the vicinity of the spacer.

INTRODUCTION

Dynamic loads on cables such as galloping, ice shedding or conductor breakage may induce high-amplitude vibrations and damaging transient dynamic forces. Spacers and spacer dampers applied on bundled conductors contribute to attenuate these vibrations. In this event, however, tension and stress peaks usually occur in the vicinity of the spacer clamps. Furthermore, if an asymmetric load acts on the bundle, then the torsion exerted on the bundle may also be significant. Asymmetric loads may arise from ice shedding from one subconductor, from non-uniform ice load on different subconductors or from the action of wind on non-uniformly iced conductor bundles. High asymmetric loads result in significant angles of rotation when the bundle becomes unstable, and it will not untwist itself after load removal [1-4]. The collapse angle at which the bundle loses its stability depends on the span parameters, and is an important issue to be determined [3-4].
The finite element method was effectively applied to model ice shedding from overhead transmission lines. Ice shedding from a single cable of a two-span section was simulated in [5] both numerically and experimentally, and this model served as a basis for developing a finite element model of ice shedding from conductor bundles [6]. This model simulates the vertical vibration of bundles, but it is not applicable to predicting the angle of bundle rotation. A four-degree-of-freedom (4DOF) model of spacers used in twin bundles was introduced in [7] to simulate both of the vertical vibration and the rotation of bundle at the spacer attachment point following ice shedding. This idea will be applied in the present paper to construct spacer models in triple and quad bundles and study their dynamics when ice sheds from one subconductor in the bundle.

Spacers in triple and quad bundles

A wide variety of spacer design has been developed by different manufacturers. However, all of them must satisfy the main requirement: keeping a constant distance between the subconductors. Spacer dampers include elastic elements; and thus, they are also applicable to attenuate cable vibration. Typical spacers consist of a rigid central frame and arms which are attached to the central frame by flexible joints, while their free ends are clamped to the subconductors. The elasticity and damping of

such spacers are based on the flexibility of the joints. Arms are allowed to rotate a few degrees around the joint with increasing resistance until the rotating part is blocked and further deformation is only possible by elongation of the spacer material. Figure 1 shows a few examples of spacers which are used in triple and quad bundles.

Figure 1: Spacers in triple and quad bundles

CONSTRUCTION OF MODEL

A 6DOF model and an 8DOF model are constructed to study the dynamics of spacers or spacer dampers in triple and quad bundles, respectively. Simplified sketches of these models can be seen in Figures 2 and 3. The conductors hang in the *y-z* plane in static equilibrium, and the spacers bring them together at mid-span in the *x-z* plane. When ice sheds from a single cable, the cable may be assumed to vibrate in the *y-z* vertical plane; however, the transverse movement cannot be neglected when spacers bring subconductors together in a bundle. The symbols m_i stand for the mass of the cables or iced cables. The index i takes the values i=1,2,3 for triple bundles, and i=1,2,3,4 for quad bundles in this discussion. The cable may be bare or iced; and, in what follows, cable properties concern cable-ice composition in case of iced cable. The elastic and damping properties of the cable and the spacer are modeled by springs and dampers, which are indicated only by lines and the symbols c_i, c_{xi}, d_i and d_{xi} in Figures 2 and 3 for the sake of simplicity. Thick continuous lines symbolize springs and dampers accounting for the stiffness and damping of the cable, whereas thick dashed lines stand for stiffness and damping of the spacer. The spacer is modeled by three and six spring-damper couples in

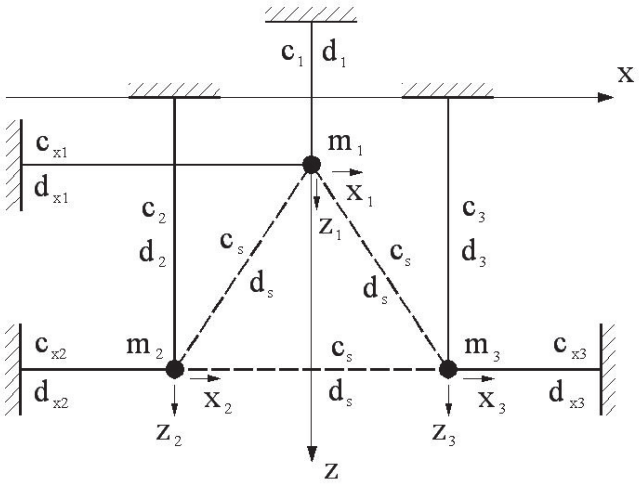

Figure 2: 6DOF model of spacer in triple bundles

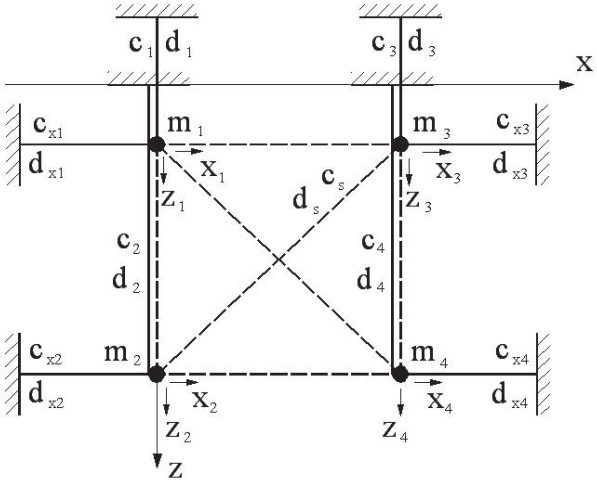

Figure 3: 8DOF model of spacer in quad bundles

triple and quad bundles, respectively. The symbols c_s and d_s are indicated only once in Figure 3 for simplicity, but all six parts of the spacer are assumed to have the same stiffness and damping. The elasticity of spacer and the elasticity of cables in the vertical direction are represented by nonlinear springs, c_s and c_i, respectively; whereas the elasticity of cables in the transverse direction are modeled by the linear springs, c_{xi}. The dampers d_i, d_{xi} and d_s account for cable damping in the vertical and transverse directions, and for spacer damping, respectively. The general coordinates of the system are the transverse, x_i, and vertical, z_i, displacements of the masses, m_i. In this section, first the mass, spring and damping constants, and then the equations of motion will be determined.

Mass of Cable and Spacer

The mass of a spacer is significantly less than that of a cable, therefore the mass of spacer is included in the mass of cable, m_i:

$$m_i = \left[\mu_i + \rho_{ice} \frac{\left(D_i + 2b_i\right)^2 - D_i^2}{4} \pi \right] L + \frac{\rho_s l_s A_s}{n} \tag{1}$$

where μ_i is the mass per unit length of bare cable, ρ_{ice} is the density of ice, D_i is the diameter of bare cable, b_i is the thickness of ice accumulation which is assumed to be circular, L is the length of the span, ρ_s, l_s and A_s are the density, length and cross-sectional area of spacer, respectively, and n is the number of subconductors in the bundle.

Spring Constants of Cable

The elastic behavior of the conductors is described by the statics of the suspended cables [8]. Ice is taken into account as a uniformly distributed load on the cable in the vertical direction. The force which acts from the spacer at the attachment point is considered as a concentrated load with vertical and transverse components. The distributed load is constant; thus, its effect is built in the cable properties. As the point load varies during the vibration, the corresponding displacement is determined by the spring characteristics, i.e. the load – displacement relationship describing cable elasticity. The details for obtaining this relationship are provided in [7]. If the vertical component of the point load is denoted by P_z, and the vertical displacement by w_p, then the vertical load – vertical displacement relationship takes the form:

$$w_p = \frac{P_z L}{4\left(\tilde{H} + h_{pz}\right)} \left(1 - \frac{\tilde{\mu} g L h_{pz}}{2 P_z \tilde{H}} \right) \tag{2}$$

where $\tilde{\mu} = \mu + \rho_{ice} \pi \left(\left(D + 2b\right)^2 - D^2 \right) / 4$, g is the gravitational constant, and $\tilde{H}$ is the initial tension of cable including the additional tension due to ice load in case of iced cable. The increment in the cable tension, h_{pz}, due to the point load is obtained from a third order equation. The $P_z - w_p$ relationship may closely be approximated by a third order polynomial in the range of w_p which arises during vibration. The vertical displacement, w_p, is exactly the general coordinate, z; and the spring force, F_{cz}, equilibrates the force, P_z, and the gravitational force, i.e. $F_{cz} = -P_z - mg$. Thus, the vertical spring force – vertical displacement relationship is defined by the following equation for each cable:

$$F_{czi} = c_{i0} + c_{i1} z_i + c_{i2} z_i^2 + c_{i3} z_i^3 \tag{3}$$

The relation between the transverse load, P_x, and transverse displacement, u_p, is obtained from:

$$u_p = \frac{P_x L}{4\left(\widetilde{H} + h_{px}\right)} \tag{4}$$

where the additional cable tension, h_{px}, due to the load, P_x, is calculated again from a third order equation, and the $P_x - u_p$ relation is approximated by a linear expression in the range of u_p which occurs during the vibration. The transverse displacement, u_p, is equal to the general coordinate, *x*; and the spring force, F_{cx}, equilibrates the force, P_x; thus, the transverse spring force – transverse displacement relationship may simply be written for each cable as:

$$F_{cxi} = c_{xi} x_i \tag{5}$$

Spring Constants of Spacer

The calculation of the spring constants accounting for the elasticity of spacer is based on [7]. In that study, a nonlinear spring was assumed to be applied between the two conductors in the twin bundle. In the present paper, the same nonlinear spring is applied between each pair of subconductors. The spring characteristics consist of a cubic function until a critical deformation is reached at the point where the rotation of the arms is blocked, and of a linear function in the region where further deformation is possible only by elongation of the spacer material:

$$F_{sij} = \begin{cases} c_{s3} \Delta l_{ij}^3 & \text{if} \quad \Delta l_{ij} < \Delta l_{cr} \\ c_{s0} + c_{s1} \Delta l_{ij} & \text{if} \quad \Delta l_{ij} \geq \Delta l_{cr} \end{cases} \tag{6}$$

The indices *ij* stand for the three couples of subconductors in case of triple bundles, and the six couples in case of quad bundles. The spring constants were determined in [7] as follows: $c_{s0} = -2E_s A_s \Delta l_{cr} / \left(3 l_s\right)$, $c_{s1} = E_s A_s / l_s$ and $c_{s3} = E_s A_s / \left(3 l_s \Delta l_{cr}^2\right)$. The elongation of the spacer, Δl_{12}, for triple bundle may be expressed by the general coordinates:

$$\Delta l_{12} = \sqrt{\left(l_s / 2 + x_1 - x_2\right)^2 + \left(z_{20} + z_2 - z_{10} - z_1\right)^2} - l_s \tag{7}$$

and, similarly, the elongations Δl_{13} and Δl_{23} for triple bundle, and Δl_{12}, Δl_{13}, Δl_{14}, Δl_{23}, Δl_{24} and Δl_{34} for quad bundle may readily be formulated according to Figure 4. The symbols z_{i0} stand for the vertical coordinate of the cables in static equilibrium when force does not act from the spacer, and Δl_{cr} is the elongation of the spacer in the limit case when the rotation of spacer arm is blocked.

The total spring forces that act at each point of mass from the spacer may be determined as a sum of the forces developing in the springs which are connected to that point of mass (see Figure 4). For triple bundles, the total spring force at mass m_1 has the form:

$$\mathbf{F}_{s1} = \left(-F_{s12} \sin\left(\pi/6 - \alpha_{12}\right) + F_{s13} \sin\left(\pi/6 + \alpha_{13}\right)\right)\mathbf{i} + \left(F_{s12} \cos\left(\pi/6 - \alpha_{12}\right) + F_{s13} \cos\left(\pi/6 + \alpha_{13}\right)\right)\mathbf{k} \tag{8}$$

The vectors **i** and **k** are unit vectors in the direction of coordinates x and z, respectively, and the angles α_{12} and α_{13} are defined in Figure 4. The trigonometric functions of $\pi/6-\alpha_{12}$ may be expressed by the general coordinates as follows:

$$\sin(\pi/6-\alpha_{12})=(l_s/2+x_1-x_2)/(\Delta l_{12}+l_s) \quad \text{and} \quad \cos(\pi/6-\alpha_{12})=(z_{20}+z_2-z_{10}-z_1)/(\Delta l_{12}+l_s) \tag{9}$$

The forces $\mathbf{F}_{s2}$ and $\mathbf{F}_{s3}$, and the trigonometric functions of the angles $\pi/6+\alpha_{13}$ and α_{23}, may be written similarly with the help of Figure 4. For quad bundles, the total spring force at mass m_1 is given by:

$$\mathbf{F}_{s1}=(F_{s12}\sin\alpha_{12}+F_{s13}\cos\alpha_{13}+F_{s14}\sin(\pi/4+\alpha_{14}))\mathbf{i}+(F_{s12}\cos\alpha_{12}-F_{s13}\sin\alpha_{13}+F_{s14}\cos(\pi/4+\alpha_{14}))\mathbf{k} \tag{10}$$

The forces $\mathbf{F}_{s2}$, $\mathbf{F}_{s3}$ and $\mathbf{F}_{s4}$, and the trigonometric functions of the angles α_{12}, α_{13}, $\pi/4+\alpha_{14}$, $\pi/4+\alpha_{23}$, α_{24} and α_{34}, are also obtained from Figure 4.

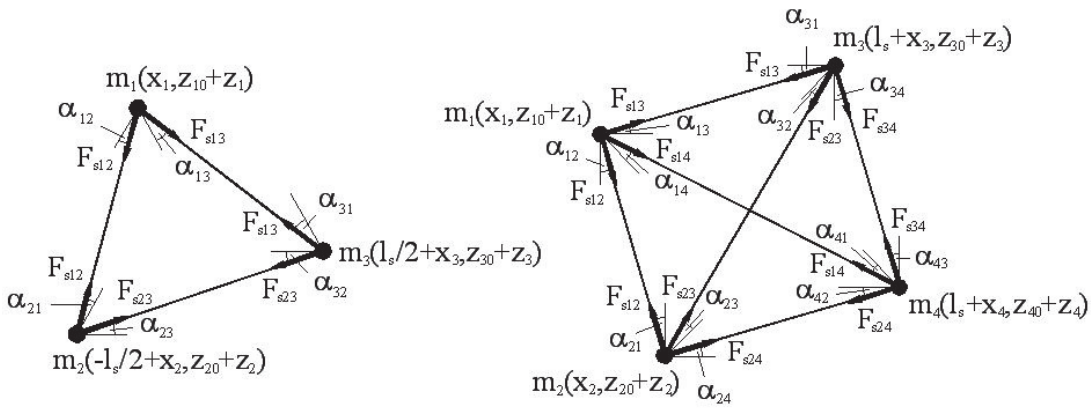

Figure 4: Spring forces acting in spacer model (angles are measured from position of spacer in static equilibrium)

Cable Damping and Spacer Damping

Cable damping forces result from structural damping and aerodynamic damping. The damping constants are calculated from the formulae:

$$d_{i1}=2\xi_i\sqrt{A_iE_i\mu_i+\left(\frac{(D_i+2b_i)^2-D_i^2}{4}\right)^2E_{ice}\rho_{ice}} \quad \text{and} \quad d_{i2}=\frac{1}{2}C_{Di}\rho A_{pi} \tag{11}$$

for structural and aerodynamic damping, respectively; where ξ_i is the damping ratio, E_{ice} is the Young's modulus of ice, C_{Di} is the drag coefficient, ρ is air density, and $A_{pi}=(D_i+2b_i)L$ is the projected area of the iced cable. Damping constants in the transverse direction, d_{xi1} and d_{xi2}, are obtained similarly. Then, the total damping force may be written as:

$$F_{dzi}=-d_{i1}\dot{z}_i-d_{i2}\dot{z}_i^2 \quad \text{and} \quad F_{dxi}=-d_{xi1}\dot{x}_i-d_{xi2}\dot{x}_i^2 \tag{12}$$

The structural damping of spacer is also considered in the model. If the spacer is assumed to be ice free, the damping constant is calculated from the formula: $d_s = 2\xi_s \sqrt{E_{s0} A_s^2 \rho_s}$, where E_{s0} is approximated as the tangent of the line drawn between the origin and the connection point of the cubic and the linear part of the stress-strain curve. Then, the damping force has the following form:

$$F_{dsij} = d_s \Delta \dot{l}_{ij} \tag{13}$$

The total damping forces that act at each point of mass from the spacer are obtained exactly in the same way as for the total spring forces, except that the spring forces F_{sij} in (8) and (10) are replaced by the damping forces F_{dsij} .

Equations of Motion

The equations of motion are determined by means of the Lagrangian equations of the second kind

$$\frac{\mathrm{d}}{\mathrm{d}t}\frac{\partial T}{\partial \dot{q}_k} - \frac{\partial T}{\partial q_k} = Q_k , \qquad k = 1,\ldots,2n \tag{14}$$

where $q_k = x_k$, $k = 1,\ldots, n$ and $q_k = z_{k-n}$, $k = n+1,\ldots, 2n$. The kinetic energy, T, and the general force, Q_k , are expressed as:

$$T = \sum_i \frac{1}{2} m_i \left(\dot{x}_i^2 + \dot{z}_i^2 \right) \qquad i = 1,\ldots, n \tag{15}$$

$$Q_k = F_{cxk} + F_{dxk} + F_{sxk} + F_{dsxk} , \quad k = 1,\ldots, n \quad \text{and}$$

$$Q_k = F_{cz,k-n} + F_{dz,k-n} + F_{sz,k-n} + F_{dsz,k-n} + m_i g , \quad k = n+1,\ldots, 2n \tag{16}$$

DYNAMIC EFFECTS OF ICE SHEDDING FROM ONE SUBCONDUCTOR

The results of simulations for different ice shedding scenarios are presented in this section. All cables are loaded with ice initially, and then full shedding is assumed from one of the cables. The ice thickness is varied through consecutive simulations between 10 mm and 60 mm. Triple- and quad-bundled Bersfort conductors are modeled with a length of 200 m and sag of 6 m. Conductor data are as follows: D = 35.6 mm, A = 747.1 mm^2 , μ = 2.37 kg/m and E = 67.6 GPa. The damping ratio of cable is assumed to be 2 %, whereas the drag coefficient is set at 1.25. The ice parameters are defined to correspond to glaze ice accretion, so that the density and Young's modulus of the ice take the values: ρ_{ice} = 900 kg/m^3 and E_{ice} = 10 GPa, respectively. The spacer material is aluminum, so that its density and Young's modulus are: ρ_s = 2700 kg/m^3 and E_s = 70 GPa, respectively. The distance between the subconductors is 0.5 m, which determines the length of spacer: l_s = 0.5 m, with the exception of the diagonal parts in the spacer for quad bundles, whose length is $\sqrt{2} l_s$. For simplification, the cross-section of spacer is cylindrical and constant, with an area of A_s = 0.0025 m^2 . The damping ratio of spacer is 20 %.

Figure 5 shows spacer positions in static equilibrium after ice sheds from one subconductor and after the vibration decays. Results for twin bundles are also presented, which are based on the simulations carried out with the model of [7]. It should be clear that the limit angle for twin and quad bundles is 90°, whereas this limit is 120° for triple bundle if we assume that the bundle does not collapse during vibration. Figure 5 shows that the rotation of bundle may be significant even in static equilibrium with an asymmetric load; the angle of rotation approaches the mentioned limits for the highest ice load.

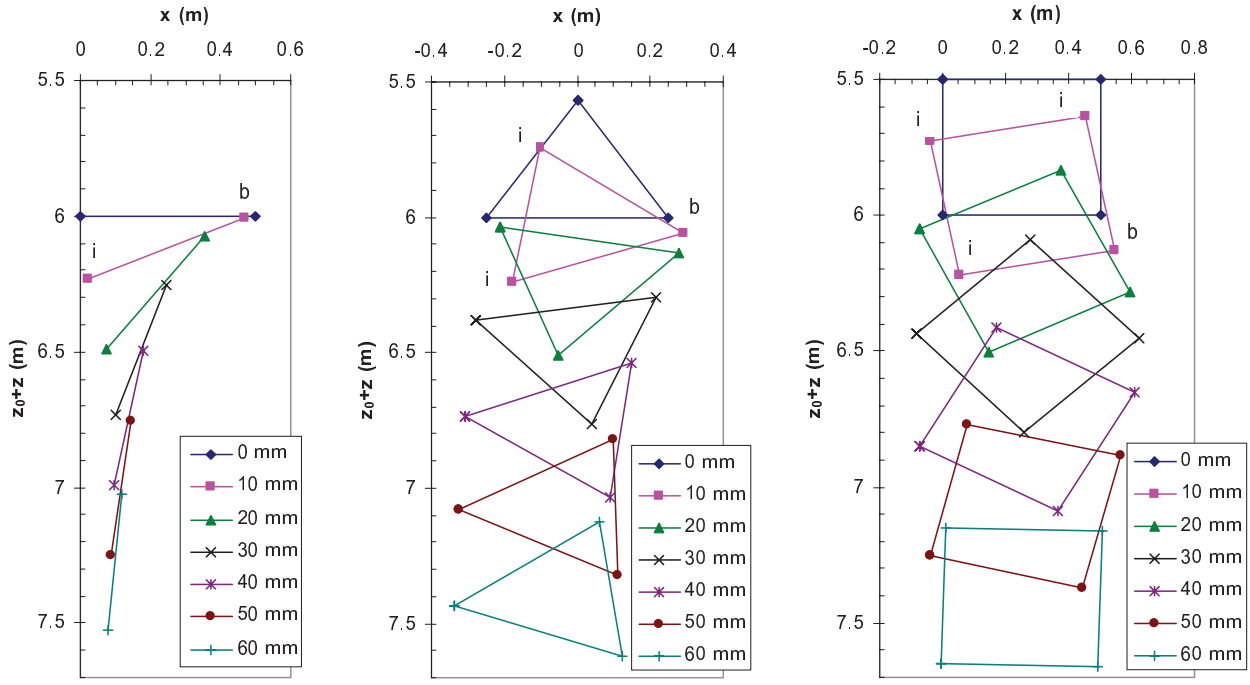

Figure 5: Spacer positions in the static equilibrium of the system when one cable is bare (b) and the other one(s) are iced (i)

Cable properties are defined in the simulations so that initially, one cable is bare while the other ones are iced. However, even the bare cable is assumed to be in the same position it would be in static equilibrium if it were covered by ice. Since this does not correspond to the equilibrium position of the bare cable, vibration is initiated. Figure 6 shows the maximum angle of rotation of the spacer and, consequently, that of the bundle at the spacer attachment during vibration for different ice thicknesses. Simulation results obtained for twin bundles in [7] are also presented, which makes it possible to compare rotation angles for twin, triple and quad bundles. According to this comparison, the maximum angle of rotation decreases with an increase in the number of subconductors. However, this angle exceeds 90° even for quad bundles when the ice load is 50 mm or higher, which means that the mid-point of the unloaded cable is pulled above that of a loaded one and that a risk of torsional instability appears (see [2-3]). In case of twin and triple bundles, this happens even for lower ice thicknesses, i.e. around 20-30 mm.

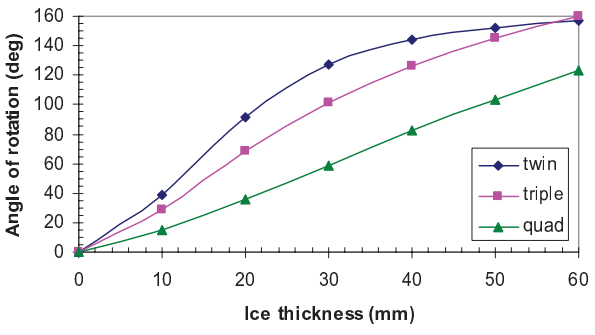

Figure 6 : Maximum angle of bundle rotation during vibration following ice shedding

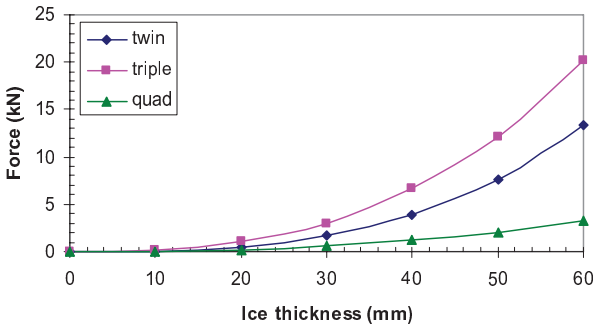

Figure 7: Maximum force acting on spacer during vibration following ice shedding

The maximum force which acts on the spacer during the vibration is presented in Figure 7. This peak force is highest for the triple bundle and lowest for the quad bundle. The results shown in Figures 6 and 7 predict that the most stable configuration is the quad bundle.

CONCLUSIONS

A model for studying the dynamic behavior of spacers and conductor bundles in the vicinity of the spacer has been developed in the present paper for triple and quad bundles. Several different ice shedding scenarios were simulated, the maximum angle of bundle rotation as well as the maximum force acting on the spacer during the resulting vibration were calculated, and the simulation results were compared to those obtained in a previous study for twin bundle. The spacer position in the static equilibrium arising after the decay of ice-shedding-induced vibration was also presented, which predicts that the rotation of spacer, and thereby that of the bundle, may be significant even in static equilibrium if the ice load is strongly asymmetric. The maximum angle of rotation during the vibration of conductor bundles approaches the value above which the bundle becomes unstable. According to the simulation results, the most stable configuration, i.e. the one with the lowest angle of rotation and lowest force developing in the spacer, is the quad bundle.

Acknowledgements

This work was carried out within the framework of the NSERC/Hydro-Québec/UQAC Industrial Chair on Atmospheric Icing of Power Network Equipment (CIGELE) and the Canada Research Chair on Engineering of Power Network Atmospheric Icing (INGIVRE) at the University of Québec at Chicoutimi. The authors would like to thank the CIGELE partners (Hydro-Québec, Hydro One, Électricité de France, Alcan Cable, K-Line Insulators, CQRDA and FUQAC) whose financial support made this research possible, as well as Mr. P. van Dyke of Hydro-Québec for the pictures of spacers.

REFERENCES

[1] Y. Matsubayashi, 1963, "Theoretical Considerations of the Twisting Phenomenon of the Bundle Conductor Type Transmission Line", *Sumimoto Electric Technical Review*, no. 1, 9-21.

[2] A. T. Edwards, J. M. Boyd, 1965, "Bundle-Conductor-Spacer Design Requirements and Development of Spacer-Vibration-Damper", *IEEE Trans. on Power Apparatus and Systems,* vol. PAS-84(10), 924-932.

[3] O. Nigol,G. J. Clarke, D. G. Havard, 1977, "Torsional Stability of Bundle Conductors", *IEEE Trans. on Power Apparatus and Systems,* vol. PAS-96(5), 1666-1674.

[4] D. G. Havard, P. van Dyke, 2005, "Effects of Ice on the Dynamics of Overhead Lines. Part II: Field Data on Conductor Galloping, Ice Shedding and Bundle Rolling", *Proceedings of 11th International Workshop on Atmospheric Icing of Structures*, Montreal, QC, Canada, 291-296.

[5] A. Jamaleddine, G. McClure, J. Rousselet, R. Beauchemin, 1993, "Simulation of Ice Shedding on Electrical Transmission Lines Using ADINA," *Computers & Structures,* vol. 47, no. 4/5, pp. 523-536, 1993.

[6] L. E. Kollár, M. Farzaneh, 2006, "Vibration of Bundled Conductors Following Ice Shedding," *IEEE Trans. on Power Delivery,* submitted.

[7] L. E. Kollár, M. Farzaneh, 2007, "Modeling Spacer Dynamics during Ice-Shedding-Induced Vibrations", *Proceedings of 12th International Workshop on Atmospheric Icing of Structures*, Yokohama, Japan, accepted.

[8] H. M. Irvine, 1981, *Cable Structures,* MIT Press, Cambridge, MA, USA.